



COVER SHEET

This is the author-version of article published as:

Frost, Ray and Xi, Yunfei and He, Hongping (2007) Modification of the surfaces of Wyoming montmorillonite by the cationic surfactants alkyl trimethyl, dialkyl dimethyl and trialkyl methyl ammonium bromides. *Journal of Colloid and Interface Science* 305(1):pp. 150-158.

Accessed from <http://eprints.qut.edu.au>

© 2007 Elsevier

Modification of the surfaces of Wyoming montmorillonite by the cationic surfactants alkyl trimethyl, dialkyl dimethyl and trialkyl methyl ammonium bromides

Yunfei Xi ^a, Ray L. Frost ^{a*} and Hongping He ^b

^a Inorganic Materials Research Group, School of Physical and Chemical Sciences, Queensland University of Technology, GPO Box 2434, Brisbane, Qld 4001, Australia

^b Guangzhou Institute of Geochemistry, Chinese Academy of Sciences, Wuashan Guangzhou 510640, China.

Abstract

Surfaces of a Wyoming SWy-2 sodium montmorillonite were modified using microwave radiation through intercalation with the cationic surfactants octadecyltrimethylammonium bromide, dimethyldioctadecylammonium bromide and methyltrioctadecylammonium bromide by an ion exchange mechanism. Changes in the surfaces and structure were characterized using X-ray diffraction (XRD), thermal analysis (TG) and Infrared (IR) spectroscopy. Different configurations of surfactants within montmorillonite interlayer are proposed based on d(001) basal spacings. A range of surfactant molecular environments within the surface-modified montmorillonite are proposed based upon their thermal decomposition. IR spectroscopy using a smart endurance single bounce diamond attenuated total reflection (ATR) cell has been used to study the changes in the spectra of CH asymmetric and symmetric stretching modes of the surfactants to provide more information of the surfactant molecular configurations.

Key words: Surfactant, organoclay, montmorillonite, adsorption, surface modification

1. Introduction

Smectites are widely used in a range of applications because of their high cation exchange capacity, swelling capacity, high surface areas, and consequential strong adsorption and absorption capacities (1-4). Among the swelling clays, the most common dioctahedral smectite is montmorillonite, which has two siloxane tetrahedral sheets sandwiching an aluminum octahedral sheet. Because of an isomorphic substitution within the layers (for example, Al^{3+} replaced by Mg^{2+} or Fe^{2+} in the octahedral sheet and Si^{4+} replaced by Al^{3+} in the tetrahedral sheet), the clay layers have permanent negative charges, which are counterbalanced by exchangeable cations such as Na^+ and Ca^{2+} in the interlayer. The hydration of inorganic cations on the exchange sites causes the clay mineral surface to be hydrophilic. Thus, natural clays are ineffective sorbents for organic compounds. The surface treatment of clay minerals has received great interests, for example, ion exchange of the inorganic cations with organic cations usually with quaternary ammonium compounds can

* Author to whom correspondence should be addressed (r.frost@qut.edu.au, Ph: +61 7 3864 2407, Fax: +61 7 3864 1804)

dramatically alter the surface properties. The intercalation of a cationic surfactant not only changes the surface properties from hydrophilic to hydrophobic but also greatly increases the basal spacing of the layers (5).

Such surface property changes will effect the applications of the organoclay. In particular, the hydrophobic nature of the organoclay implies that the material can be used as a filter material for water purification through for example the removal of hydrocarbons and pesticides. At present, there are many applications of organoclays used as sorbents in pollution prevention and environmental remediation such as the treatment of spills, in wastewater and hazardous waste landfills, and others. Some studies have shown that replacing the inorganic exchangeable cations of clay minerals with organic cations can result in a greatly enhanced capacity of these materials to remove organic contaminants (6,7). Organoclay based nanocomposites exhibit a remarkable improvement in properties when compared with untreated polymer or conventional micro- and macro-composites. These improvements include increased strength and heat resistance, decreased gas permeability and flammability, and increased biodegradability of biodegradable polymers (8, 9). All of these applications and improvements mentioned above strongly depend on the structure and properties of the organoclays. Understanding the structure and properties of organoclays is essential for their industrial applications.

The objective of this study is to investigate the surface modification of a Wyoming montmorillonite with a series of differently structured surfactants namely octadecyltrimethylammonium bromide (ODTMA), dimethyldioctadecylammonium bromide (DMDOA) and trioctadecylmethylammonium bromide (TOMA). The concentration of these surfactants was varied from 0.2 CEC to 2.0 CEC. X-ray diffraction (XRD), Fourier transform infrared spectroscopy (FTIR) and thermogravimetric analysis (TG) were used to probe the microenvironment and packing arrangement of organic surfactant within the organoclays. This study provides new insights into the structure and properties of organoclays prepared by microwave. Such a study is of high importance for understanding the structure, properties, and potential applications of organoclays.

2. Experimental section

2.1 Materials.

The montmorillonite used in this study was supplied by the Clay Minerals Society as source clay SWy-2-Na-montmorillonite (Wyoming). This clay originates from the Newcastle formation, (cretaceous), County of Crook, State of Wyoming, USA. The chemical composition of the montmorillonite is: SiO₂ 62.9%, Al₂O₃ 19.6%, Fe₂O₃ 3.35%, MgO 3.05%, CaO 1.68%, Na₂O 1.53%. The formula of the montmorillonite can be expressed as (Ca_{0.12} Na_{0.32} K_{0.05})[Al_{3.01} Fe(III)_{0.41} Mn_{0.01} Mg_{0.54} Ti_{0.02}][Si_{7.98} Al_{0.02}]O₂₀(OH)₄, as calculated from its chemical composition. The cation exchange capacity (CEC) is 76.4 meq/100g. The clay was used without further purification. The surfactants selected for this study are octadecyltrimethylammonium bromide (C₂₁H₄₆NBr, FW: 392.52), dimethyldioctadecylammonium bromide (C₃₈H₈₀BrN, MW: 630.95) and methyltrioctadecylammonium bromide (C₅₅H₁₁₄BrN, MW: 869.40) and were used as supplied by Sigma-Aldrich.

2.2 Preparation of surfactant modified montmorillonites

2g of SWy-2-Na-montmorillonite (denoted as SWy-2-MMT) was dispersed in a solution of pre-dissolved stoichiometric amount of surfactant (surfactant dissolved in 80ml deionized water + 80ml ethanol solution) under stirring for 10min. The clay and surfactant mixture was poured into a set of sealed Teflon microwave reaction container with temperature/pressure probes and then put into a Milestone Microwave Laboratory System(10). The temperature of the mixture was increased from room temperature to 140 °C within 20min with a microwave output <510watt, then kept in 140 °C (5.3 bar) for another 20min with an output of 400 watt. The mixture was stirred with magnetic stirrer fitted in the system during the whole procedure.

The surfactants are octadecyltrimethylammonium bromide (denoted as ODTMA), dimethyldioctadecylammonium bromide (denoted as DMDOA) and trioctadecylmethylammonium bromide (denoted as TOMA). The concentrations of surfactants used are 0.2 CEC (Cation Exchange Capacity), 0.4 CEC, 0.6 CEC, 0.8 CEC, 1.0 CEC and 2.0 CEC of the SWy-2-MMT. All organoclays were washed free of bromide anions as determined by the use of AgNO₃, dried at room temperature and ground in an agate mortar, and stored in a vacuum desiccator. The ODTMA, DODMA and TOMA modified montmorillonite prepared at a concentration of 0.2 CEC were denoted as OM0.2CEC, DM0.2CEC and TM0.2CEC respectively, and the others were denoted in a similar way.

2.3 X-ray diffraction.

The SWy-2-MMT and organoclays were pressed in stainless steel sample holders. X-ray diffraction (XRD) patterns were recorded using CuK α radiation ($\lambda = 1.5418\text{\AA}$) on a Philips PANalytical X' Pert PRO diffractometer operating at 40 kV and 40 mA with 0.125° divergence slit, 0.25° anti-scatter slit, between 3 and 15° (2 θ) at a step size of 0.0167°. For XRD at lower angle section, it was between 1 and 5° (2 θ) at a step size of 0.0167° with automatic variable divergence slit and 0.5° anti-scatter slit.

2.4 Infrared spectroscopy.

Infrared (IR) spectra were obtained using a Nicolet Nexus 870 FTIR spectrometer with a smart endurance single bounce diamond ATR cell. Spectra over the 4000–525 cm⁻¹ range were obtained by the co-addition of 64 scans with a resolution of 4 cm⁻¹ and a mirror velocity of 0.6329 cm s⁻¹. Spectral manipulation such as baseline adjustment, smoothing and normalisation was performed using the GRAMS® software package (Galactic Industries Corporation, Salem, NH, USA).

2.5 Thermogravimetric analysis.

Thermogravimetric analyses of the surfactant-modified montmorillonites were obtained using a TA Instruments Inc. Q500 high-resolution TGA operating at a ramp of 10 °C/min with a resolution of 6.0 °C from room temperature to 1000 °C in a high-purity flowing nitrogen atmosphere (80 cm³/min). Approximately 50 mg of the finely ground sample was heated in an open platinum crucible. Repetitive analyses were undertaken.

3. Results and discussion

3.1 X-ray diffraction.

The modification of the montmorillonite by cation exchange reaction with cationic surfactants (with one, two or three C18 chains respectively) through their incorporation into the interlayer space can be followed through the expansion of the montmorillonitic clay. Figure 1 shows the XRD patterns of untreated SWy-2-MMT and ODTMA modified MMTs. As our previous study showed (4), there are two reflections at around 24 Å and 12 Å for SWy-2-MMT. The later should be attributed to the basal spacing of sodium montmorillonite while the former reflects a “supercell or superlayer”, resulting from the packing arrangement of neighbouring layers. Figure 1 shows the XRD patterns of these organoclays with added surfactant ODTMA amount at 0.2 CEC, 0.4 CEC, 0.6 CEC, 0.8 CEC, 1.0 CEC and 2.0 CEC. With the cation exchange of the sodium ion by the cationic surfactant, expansion of the montmorillonite layers is observed: OM0.2CEC and OM0.4CEC display a peak at 14.4 Å and 14.65 Å, in accordance with our previous study (3). With the surfactant concentration increased to 0.6 CEC, double overlapping peaks at 17.75 Å and 14.56 Å respectively are observed which shows a transition of surfactant arrangements. OM0.8CEC shows peak at 18.23 Å and OM1.0CEC a peak at 19.03 Å, while OM2.0CEC displays a peak at 21.38 Å with a shoulder at 19.54 Å.

From the literature (11), the TOT layer (tetrahedral + octahedral + tetrahedral) thickness of montmorillonite is 9.7 Å. According to the calculation of molecular size based on the data of van der Waals radius, covalent bond radius and bond angle, in case of the HDTMA, when it lies stretched out, the shape of the molecular looks like a “nail” consisting of the ‘nail-head’ (4.3 Å, four methyl groups connected with a N atom) and ‘nail-body’ (21 Å, long alkyl chain which has 15 C)(1). According to this calculation, the size of ODTMA should be 23.8 Å for “nail-body” and 4.3 Å for “nail-head”, so the full length of ODTMA will be 28.1 Å. From the transverse view, the height dimensions of the “nail-body” and “nail-head” are 4.6 Å and 5.1 Å respectively when the plane of the zigzag arranged chain of ODTMA is perpendicular to the plane of the layer. While these values will be 4.1 Å and 6.7 Å when the plane of chain takes parallel arrangement to the silicate plane(1).

Depending on charge density and different concentration of surfactant, ODTMA in OM0.2CEC and OM0.4CEC takes a lateral monolayer arrangement in the interlayer space of montmorillonite. OM0.6CEC shows the transition status varying from lateral monolayer to lateral bilayer arrangements demonstrating property variation (e.g. surface charge density) among montmorillonite layers. Interlayer surfactant in OM0.8CEC takes arrangements of lateral bilayers. The organoclay prepared with 1.0 CEC ODTMA shows a basal spacing of 19.03 Å corresponding to a bilayer arrangement, which is even larger than that of a 1.4 CEC concentration modified clay by microwave methods which has a basal spacing of 17.7 Å (12). For OM2.0CEC, it shows a basal spacing at 21.38 Å with a shoulder at 19.54 Å reflecting arrangements from bilayer to paraffin-type monomolecular.

For organoclays prepared with surfactant DODMA which has two octadecyl chains, larger basal spacing can be observed as shown in Figure 2. DM0.2CEC shows double overlapping peaks at 22.1 Å, 15 Å and a small shoulder at about 12 Å (not shown) respectively with the intensity of latter peak (15 Å) stronger. It is postulated that the basal spacing at 15 Å is corresponding to lateral monolayers. However, since the bigger space size of two long C18 chains which makes the basal spacing larger than that in ODTMA modified clays and the peak at 22.1 Å should correspond to

paraffin-type monomolecular arrangement which means the alkyl chains assume a tilted upright position to the aluminosilicate surface. For DM0.4CEC, there are several peaks observed at 23.18 Å, 19.44 Å (shoulder), 14.71 Å (not shown) and 12.03 Å (not shown). The peaks at 14.71 Å and 23.18 Å reflect arrangements from lateral monolayer to paraffin-type monomolecular. The latter peak is stronger in intensity which means paraffin-type monomolecular arrangement takes bigger portion in this organoclays. DM0.6CEC shows peak at 24.69 Å, 14.87 Å (not shown) and 12.57 Å (not shown), which presents paraffin-type monomolecular with larger tilt angle of carbon chains, however monolayer arrangement still exists.

Peaks at 25.6 Å and 12.87 Å (not shown) were observed for DM0.8CEC, it can be concluded that the tilt angle increases further when higher surfactant concentration is reached. DM1.0CEC shows peak at 26.11 Å and 12.89 Å (not shown) presenting paraffin-type monomolecular arrangements, this basal spacing is larger than reported which showed 23.9 Å (13). When the concentration of surfactant was increased to 2.0 CEC, there are a series of peaks observed, they are peaks at 39.83 Å (001) with a shoulder at 32.9 Å, 22 Å, 20.1 (002) Å and 13.32 Å (not shown). The peak at 32.9 Å corresponds to a paraffin-type bilayer arrangements since the basal spacing for a fully vertical 18C chain is at most as long as 37.8 Å (28.1 + 9.7 Å) where 28.1 Å is the full length of a 18 C chain. The peaks at 32.9 and 22 Å are in a paraffin-type monomolecular arrangement, but the tilt angle is bigger for the former. In addition, in these organoclays, there are peaks observed at about 12 Å to 13 Å, it shows that some layers are kept unaltered, indicating the steric effect of DODMA has taken into effect.

For organoclays prepared by surfactant TOMA which has three octadecyl chains, there are more peaks for each sample. Because of the larger size of the three octadecyl chains in TOMA (steric effect), some basal spacings at about 12 Å can be found for almost all the concentration loaded samples which are very close to 11.37 Å (untreated SWy-2-MMT). This reveals that some layers of the MMT are unaltered because of the steric effect arising from the relative larger surfactant molecule which has three 18 C chains. As shown in Figure 3, TM0.2CEC shows peaks at 28.2 Å with a shoulder at 21.36 Å and another peak at 15.18 Å (not shown), corresponding to arrangements of paraffin-type monolayer and a structure similar to lateral monolayer, respectively. However the larger size of TOMA makes the latter basal spacing larger than other relative smaller surfactant modified clays. TM0.4CEC shows peaks at 32.45 Å (001), 21.61 Å and 14.98 Å (not shown), while TM0.6CEC shows peaks at 33.36 Å (001), 20.82 Å, 14.98 Å (not shown) and 12.15 Å (not shown). TM0.8CEC shows peaks at 34.18 Å (001) with a shoulder at 20.24 Å, 17.46 Å (002) and 12.01 Å (not shown). TM1.0CEC shows peaks at 35.14 Å (001) and 17.60 Å (002) and 11.78 Å (not shown), again the basal spacing at 35.14 Å is larger than that in literature which showed 33.8 Å for TOMA modified montmorillonite (13). And TM2.0CEC shows peaks at 35.66 Å (001), 17.74 Å (002), 11.75 Å with tiny shoulder at 11.16 Å (not shown). The gradually increased basal spacing reflects the increase of the tilt angle of surfactants in these organoclays. For TM1.0CEC and TM2.0CEC, it can be concluded that the chains may stand up completely with tilt angle at about 90 degrees (vertical to the layer surface). It also can be concluded that the larger space size of TOMA to some extent has prohibited it from intercalating into layers which makes the basal spacing of TOMA modified clay even smaller than that of DODMA modified ones in higher surfactant loadings, for example, the basal spacings of TM2.0CEC and DM2.0CEC are 35.56 and 39.68 Å respectively. This conclusion is different from that

reported in literature where larger basal spacing was shown in TOMA modified clay than that in DODMA modified clay(13).

3.2 Thermogravimetric analysis

The decomposition procedure of pure surfactant DODMA is very different from that of ODTMA. The latter has only one surfactant decomposition peak at 196 °C as shown in Figure 4, while the former has at least three peaks at 164 °C, 244 °C and 302 °C respectively (see Figure 5). It demonstrates that for surfactant with two C18 chains, the decomposition takes place in several steps. For surfactant TOMA (as shown in Figure 6), it has similar behaviour which shows decomposition peaks of pure surfactant at 159 °C, 271 °C and 317 °C respectively. The decomposition procedure of ODTMA modified clays has been discussed in our previous study (3), while in this study the organoclays prepared by microwave methods did not show any obvious difference in the decomposition procedure of surfactants.

In Figure 5, DM0.2CEC shows peak at 362 °C with two shoulders at 274 °C and 314 °C respectively, while DM0.4CEC shows a sharp peak at 286 °C and a small peak at 338 °C. When the concentration of surfactant was increased to 0.6 CEC, it shows a peak at 278 °C with a shoulder at 345 °C. And when the concentration of surfactant was increased further, the temperature of the peak which is at 278 °C will drop down to 265 °C and there is a shoulder appearing at about 299 °C, the previous shoulder (at 345 °C) has evolved into a peak and the temperature has increased to 382 °C. The DTG curve of DM0.8CEC show two main decomposition peaks and the one at ca. 266 °C displays two shoulders. This is different from the conclusion obtained by Maged et al (14), where only one decomposition peak was observed. The implication of two peaks in the DTG analysis is indicative of two different structures in the organoclay. Such observations are also seen in the TG patterns of the higher surfactant loaded organoclays. When surfactant concentration reached 1 CEC and 2 CEC, four peaks can be observed, i.e., they are at 232 °C, 266 °C, 328 °C and 378 °C respectively for DM1.0CEC and 175 °C, 221 °C, 330 °C and 382 °C respectively for DM2.0CEC. Generally speaking, the TG results are much more complicated for DODMA modified clays than those of ODTMA modified ones.

In Figure 6, TM0.2CEC shows two peaks, one at 320 °C with a shoulder centred at ca. 255 °C and the other one at 358 °C. TM0.4CEC shows peaks at 327 °C and 366 °C respectively, and TM0.6CEC shows two main decomposition peaks at 331 °C (with a shoulder at ca. 278 °C) and 377 °C respectively. TM0.8CEC shows peaks at 316 °C (a shoulder at ca. 269 °C) and 400 °C respectively. TM1.0CEC and TM2.0CEC show four peaks at 213 °C, 268 °C, 332 °C and 404 °C respectively for the former and at 169 °C, 296 °C, 346 °C and 408 °C respectively for the latter. From TG results of DODMA and TOMA modified clays, it is hard to describe different surfactant molecular environments as what has been observed in ODTMA modified clays (3). However, it is very obvious that, for DODMA and TOMA modified montmorillonites, before the concentration reaches 2 CEC, there is not any peak at about 200 °C which comes from the decomposition of the external surface sorbed surfactant. This indicates that the intercalation of surfactant into clay interlayer space results in an increase of the thermal stability of surfactant.

As shown by XRD patterns and TG curves, the surfactants have been successfully intercalated into clay interlayers or on the surface of SWy-2-MMT. There may be differences between the amounts of surfactant added and loaded. The loaded surfactant amount could be determined by thermogravimetry (TG). According to Equation 1, the loaded amount of the surfactants could be calculated, and the results are listed in Table 1.

$$X = \frac{m \cdot S \cdot 10^{-2} \cdot 100}{(M-y) \cdot m \cdot (100-S) \cdot 10^{-2} \cdot 76.4 \cdot 10^{-3}} = \frac{S \cdot 10^5}{76.4 \cdot (M-y) \cdot (100-S)} \quad \text{Equation 1}$$

$$X = \frac{m \cdot S \cdot 10^{-2} \cdot 100}{(M-y) \cdot m \cdot (100-S) \cdot 10^{-2} \cdot 76.4 \cdot 10^{-3}} = \frac{S \cdot 10^5}{76.4 \cdot (M-y) \cdot (100-S)}$$

Where X is the loaded surfactant amount; m is the total weight of organoclay; M is the molecular weight of surfactant; S% is the weight loss percentage of surfactant in organoclay; y is 0 (if all the Br ions remain) or 80 (no Br ion, the molecular weight of Br is 80), y = 0 or 80 is not possible to reach but it can help to work out the range of X by calculating theoretical maximum and minimum values.

Table 1 shows that there are differences between the amount of surfactant added and the amount of surfactant loaded in organoclay. It is obvious in ODTMA and DODMA modified organoclays that there is less surfactant loaded in the clays than that predicted by the theoretical values (Figures 7 and 8). For organoclay prepared using TOMA, as shown in Figure 9, the data fits quite well to the theoretical values except at 0.8 CEC concentration.

3.3 Infrared Spectroscopy

It has been proven that FTIR spectroscopy is a sensitive tool to probe the molecular environment of the intercalated surfactant within the organoclay. Our previous study proposed that the frequency of CH₂-stretching mode of amine chains is extremely sensitive to the conformational ordering of the chains (15). The bands at ~2930 and ~2850 cm⁻¹ are attributed to CH₂ antisymmetric stretching vibration ν_{as} (CH₂) and symmetric stretching vibration ν_s (CH₂) respectively and they were found to be sensitive to changes in the gauche/trans conformer ratio and the chain-chain interactions.

For ODTMA modified montmorillonite, as the loading of surfactant increases from 0.2 CEC to 0.4, 0.6, 0.8, 1.0 and 2.0 CEC, ν_{as} (CH₂) shifts from 2927 cm⁻¹ for OM0.2CEC to 2922 cm⁻¹ for OM2.0CEC (Figure 10). In general, the frequency of ν_{as} (CH₂) is sensitive to the gauche/trans conformer ratio and the packing density of methylene chains (16, 17). Band shifts to higher wavenumbers is characteristic of disorder gauche conformations. The band shifts to lower wavenumbers is characteristic of highly ordered all-trans conformations. Generally speaking, with the increase of surfactant loading, the frequency of ν_{as} (CH₂) decreases. However, some fluctuations can be found, the frequency of ν_{as} (CH₂) decreases from OM0.2CEC to OM0.4CEC, while from OM0.4CEC to OM1.0CEC, the frequency remains constant

at 2926 cm^{-1} , then it decreases from 2926 cm^{-1} to 2922 cm^{-1} for OM1.0CEC and OM2.0CEC. The frequency of $\nu_{\text{as}}(\text{CH}_2)$ in all the organoclays is higher than that in pure surfactant which is at 2916 cm^{-1} , reflecting that the surfactants in organoclays take some disordered conformations comparing to that in pure surfactant.

For the DODMA modified clays as shown in Figure 11, the frequency decreases from 2926 cm^{-1} for DM0.2CEC to 2924 cm^{-1} for DM0.4CEC, then it remains constant at 2922 cm^{-1} for DM0.6CEC and DM0.8CEC, and the wavenumber decreases again to 2920 cm^{-1} for DM1.0CEC. While for DM2.0CEC, the antisymmetric stretching band has same frequency as that of pure surfactant. At this concentration it is probable that so much surfactant is adsorbed on the surface that the value of the antisymmetric stretching vibration corresponds with that of the pure surfactant. The antisymmetric CH_2 stretching vibration (ν_{as}) of TM0.2CEC shifts from 2924 cm^{-1} to 2920 cm^{-1} for TM0.4CEC (Figure 12). Both TM0.6CEC and TM0.8CEC have same frequencies which are at 2918 cm^{-1} . For TM1.0CEC and TM2.0CEC, this band can be observed waving from 2916 to 2918 cm^{-1} while pure TOMA shows the antisymmetric vibration $\nu_{\text{as}}(\text{CH}_2)$ at 2914 cm^{-1} .

Here, it can be found that the frequency shift of CH_2 stretching vibrations can be used as a guide to determine the molecular environment of the surfactant molecules in the organoclay interlayer. The higher frequencies (disorder gauche conformation) represent a liquid-like environment of surfactant while the lower frequencies represent a solid-like environment of the surfactant within the montmorillonite layers.

4. Conclusions

Based on the basal spacings from the XRD patterns, a model of surfactant configuration is proposed as a function of surfactant concentration to give details of molecular arrangement within the clay interlayer space. It is shown that, for ODTMA modified montmorillonites, microwave preparation method assists efficiently the organoclay synthesis. The configurations of these organoclays are the same as those prepared by other methods. For DODMA and TOMA modified clays, since the larger sizes of the surfactants, some layers of montmorillonite are kept unaltered because of steric effects. The configurations of surfactant within these organoclays usually take paraffin type arrangements and in some organoclays with higher surfactant loadings, the tilt angle of surfactant molecule can reach about 90° , i.e., the surfactant molecules stand up vertically within the interlayer.

The utilization of HRTG allows one to determine the thermal behaviour of organoclays prepared by surfactants with different numbers of alkyl chains and to provide information on their configuration and structural changes. It is shown that the decomposition procedure of DODMA and TOMA modified clays are very different from that of ODTMA modified ones. The surfactant decomposition takes place in several steps in the DODMA and TOMA modified clays while for ODTMA modified clays, it shows only one step for the decomposition of surfactant. TG was also proved to be a useful tool to estimate the amount of surfactant within the organoclays. FTIR was used as a guide to determine the phase state of the organoclay interlayers as determined from the CH_2 stretching vibrations of the surfactants. With the increase

of the loaded surfactant, the local environment of the loaded surfactant varies from a “liquid-like” state (disordered gauche conformation) to a “solid-like” state (ordered all-trans conformation).

Acknowledgements

The financial and infra-structure support of the Queensland University of Technology Inorganic Materials Research Program of the School of Physical and Chemical Sciences is gratefully acknowledged. The Australian Research Council (ARC) is thanked for funding through a linkage project. The Queensland Main Roads Department is thanked for funding this research.

References

1. He, H., Frost, R. L., Bostrom, T., Yuan, P., Duong, L., Yang, D., Xi, Y. and Klopprogge, J. T., *Applied Clay Science* **31**, 262 (2006).
2. He, H. P., Ding, Z., Zhu, J. X., Yuan, P., Xi, Y. F., Yang, D. and Frost, L. R., *Clays and Clay Minerals* **53**, 287 (2005).
3. Xi, Y., Ding, Z., He, H. and Frost, R. L., *Journal of Colloid and Interface Science* **277**, 116 (2004).
4. Xi, Y., Frost, R. L., He, H., Klopprogge, T. and Bostrom, T., *Langmuir* **21**, 8675 (2005).
5. Boyd, S. A., Shaobai, S., Lee, J.-F. and Mortland, M. M., *Clays and Clay Minerals* **36**, 125 (1988).
6. Mortland, M. M., Shaobai, S. and Boyd, S. A., *Clays and Clay Minerals* **34**, 581 (1986).
7. Smith, J. A., Jaffe, P. R. and Chiou, C. T., *Environmental Science and Technology* **24**, 1167 (1990).
8. Gilman, J. W., *Applied Clay Science* **15**, 31 (1999).
9. Lebaron, P. C., Wang, Z. and Pinnavaia, T. J., *Applied Clay Science* **15**, 11 (1999).
10. Klopprogge, J. T., Weier, M. L., Duong, L. V. and Frost, R. L., *Materials Chemistry and Physics* **88**, 438 (2004).
11. Harris, D. J., Bonagamba, T. J. and Schmidt-Rohr, K., *Macromolecules* **32**, 6718 (1999).
12. Baldassari, S., Komarneni, S., Mariani, E. and Villa, C., *Applied Clay Science* **31**, 134 (2006).
13. Osman, M. A., Ploetze, M. and Skrabal, P., *Journal of Physical Chemistry B* **108**, 2580 (2004).
14. Osman, M. A., Ernst, M., Meier, B. H. and Suter, U. W., *Journal of Physical Chemistry B* **106**, 653 (2002).
15. Xi, Y., Ding, Z., He, H. and Frost, R. L., *Spectrochimica Acta, Part A: Molecular and Biomolecular Spectroscopy* **61A**, 515 (2005).
16. Li, Y. and Ishida, H., *Langmuir* **19**, 2479 (2003).
17. Venkataraman, N. V. and Vasudevan, S., *Journal of Physical Chemistry B* **105**, 1805 (2001).

List of Figures

Figure 1 X-ray diffraction patterns of ODTMA modified SWy-2-MMT samples.

Figure 2 X-ray diffraction patterns of DODMA modified SWy-2-MMT samples

Figure 3 X-ray diffraction patterns of TOMA modified SWy-2-MMT samples

Figure 4 TG and DTG results of ODTMA modified clays

Figure 5 TG and DTG results of DODMA modified clays

Figure 6 TG and DTG results of TOMA modified clays

Figure 7 Real surfactant loading in ODTMA modified clays
(solid circle represents theoretical CEC values; rectangle represents real CEC value when all Br ions remained in surfactant; triangle represents real CEC value when no Br ions remained in surfactant).

Figure 8 Real surfactant loading in DODMA modified clays
(solid circle represents theoretical CEC values; rectangle represents real CEC value when all Br ions remained in surfactant; triangle represents real CEC value when no Br ions remained in surfactant).

Figure 9 Real surfactant loading in TOMA modified clays
(solid circle represents theoretical CEC values; rectangle represents real CEC value when all Br ions remained in surfactant; triangle represents real CEC value when no Br ions remained in surfactant).

Figure 10 Asymmetric and symmetric stretching vibrations of CH₂ in ODTMA modified clays

Figure 11 Asymmetric and symmetric stretching vibrations of CH₂ in DODMA modified clays

Figure 12 Asymmetric and symmetric stretching vibrations of CH₂ in TOMA modified clays

List of Tables

Table 1 Real surfactant loading in the synthesized organoclays

Table 2 Wavenumber shift of CH₂ asymmetric stretching vibration

CEC (added)	0.2	0.4	0.6	0.8	1	2
ODTMA-SWy-2-MMT						
S	4.883	7.671	13.730	15.790	20.380	25.040
Exchanged value (with Br ion)	0.171	0.277	0.531	0.625	0.854	1.114
(without Br ion)	0.215	0.348	0.667	0.785	1.072	1.399
DODMA-SWy-2-MMT						
S	8.407	11.070	14.860	24.820	31.300	48.900
Exchanged value (with Br ion)	0.190	0.258	0.362	0.685	0.945	1.985
(without Br ion)	0.218	0.296	0.415	0.784	1.082	2.273
TOMA-SWy-2-MMT						
S	11.200	20.010	28.220	31.130	38.980	56.650
Exchanged value (with Br ion)	0.190	0.377	0.592	0.681	0.962	1.967
(without Br ion)	0.209	0.415	0.652	0.749	1.059	2.167

Table 1 Real surfactant loading of ODTMA, DODMA and TOMA in the synthesized organoclays

	OM	DM	TM
CEC			
0.2	2927	2926	2924
0.4	2926	2924	2920
0.6	2926	2922	2918
0.8	2926	2922	2918
1	2926	2920	2916
2	2922	2916	2918
Pure ODTMA	2916	Pure DODMA	2916
		Pure TOMA	2914

Table 2 Wavenumber shift of CH₂ asymmetric stretching vibration

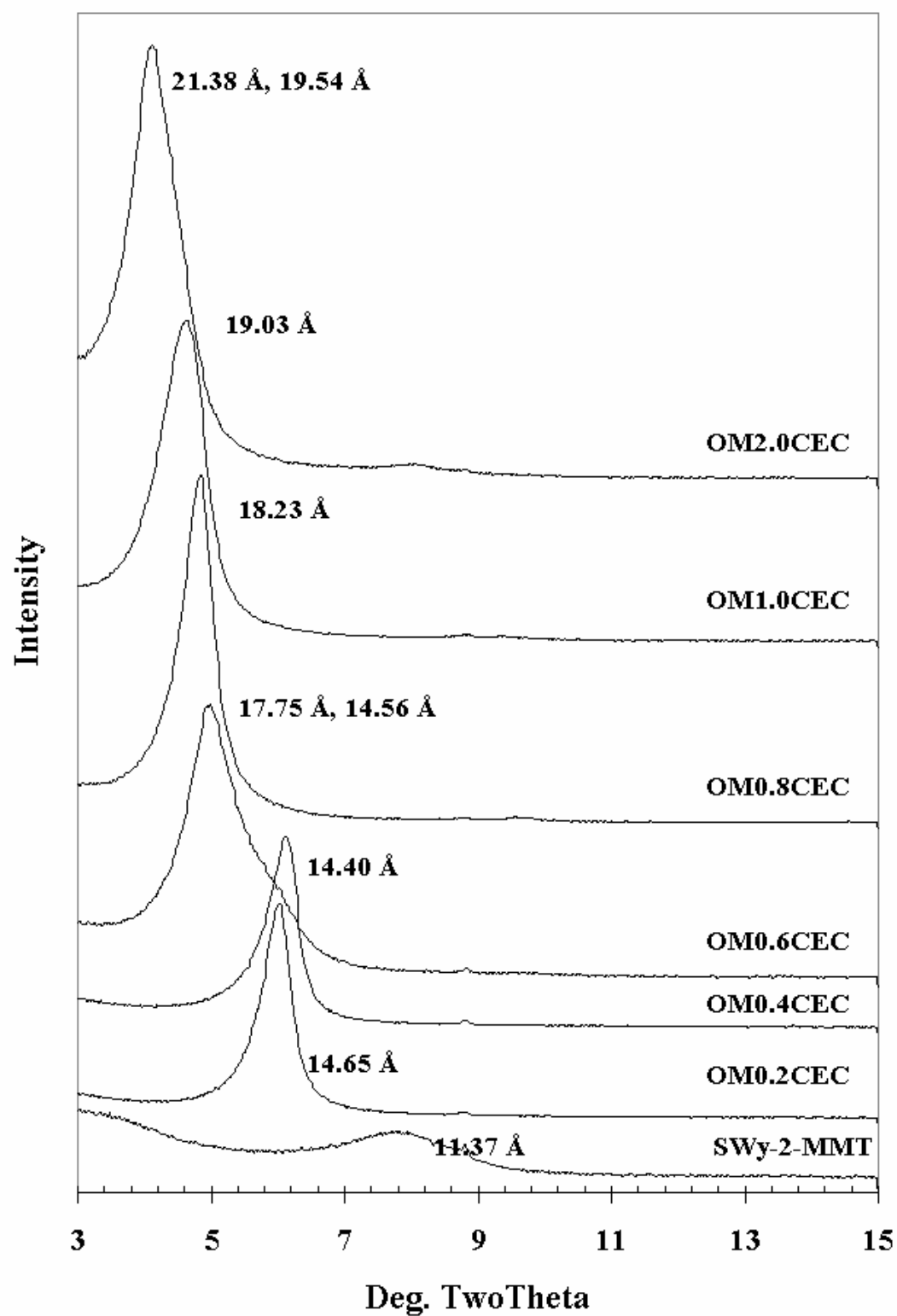


Figure 1 X-ray diffraction patterns of ODTMA modified SWy-2-MMT samples

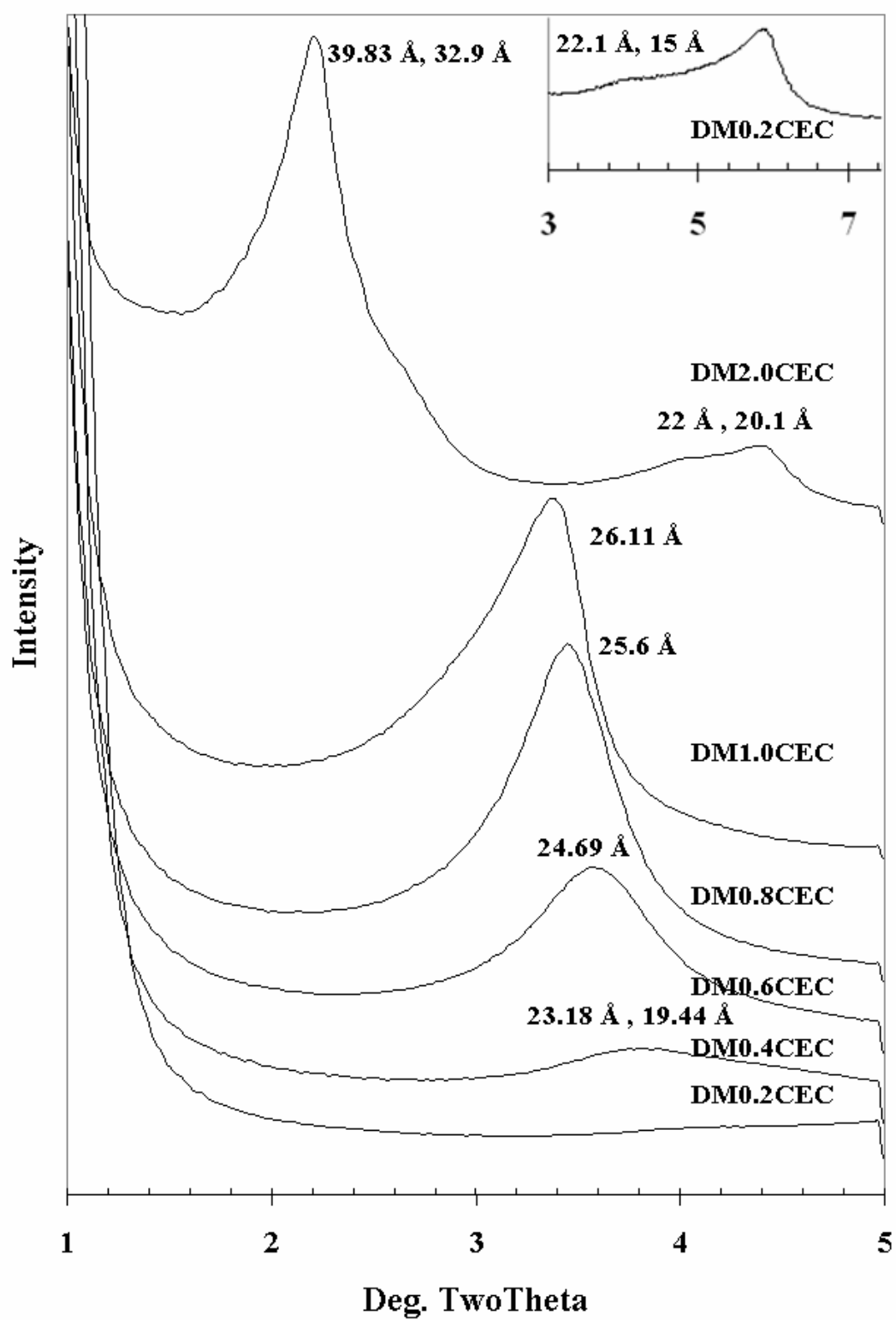


Figure 2 X-ray diffraction patterns of DODMA modified SWy-2-MMT samples

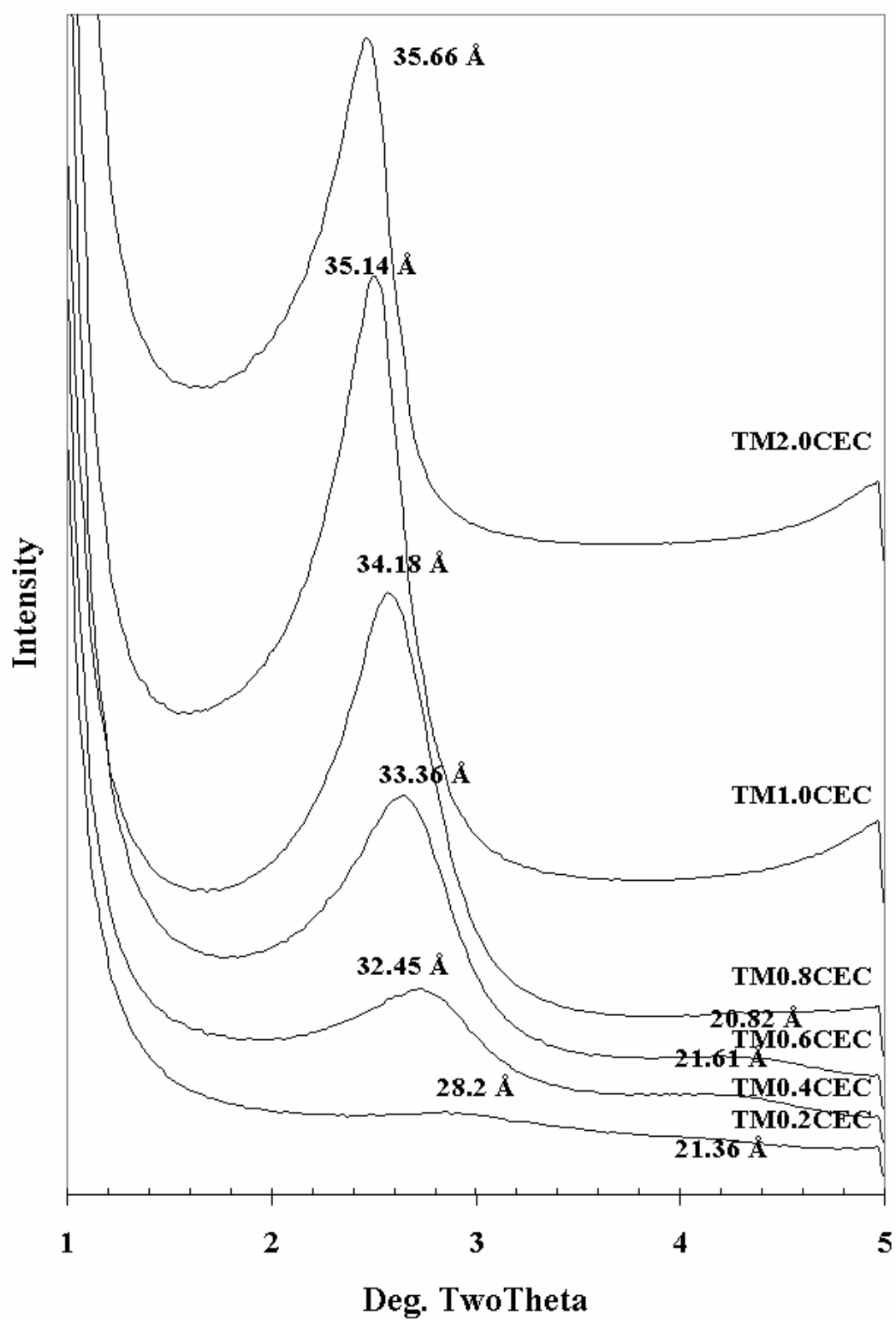


Figure 3 X-ray diffraction patterns of TOMA modified SWy-2-MMT samples

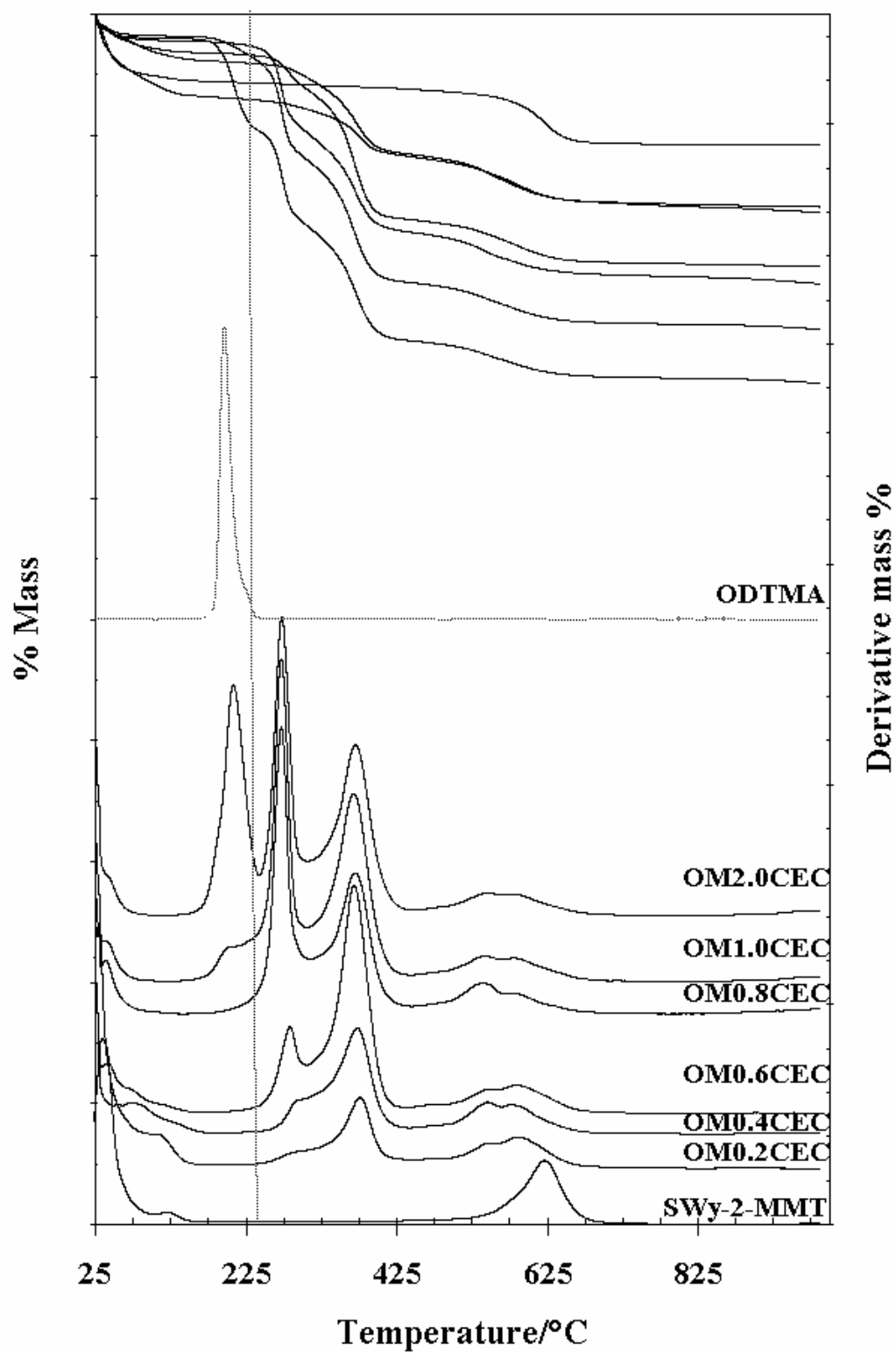


Figure 4 TG and DTG curves of ODTMA modified clays

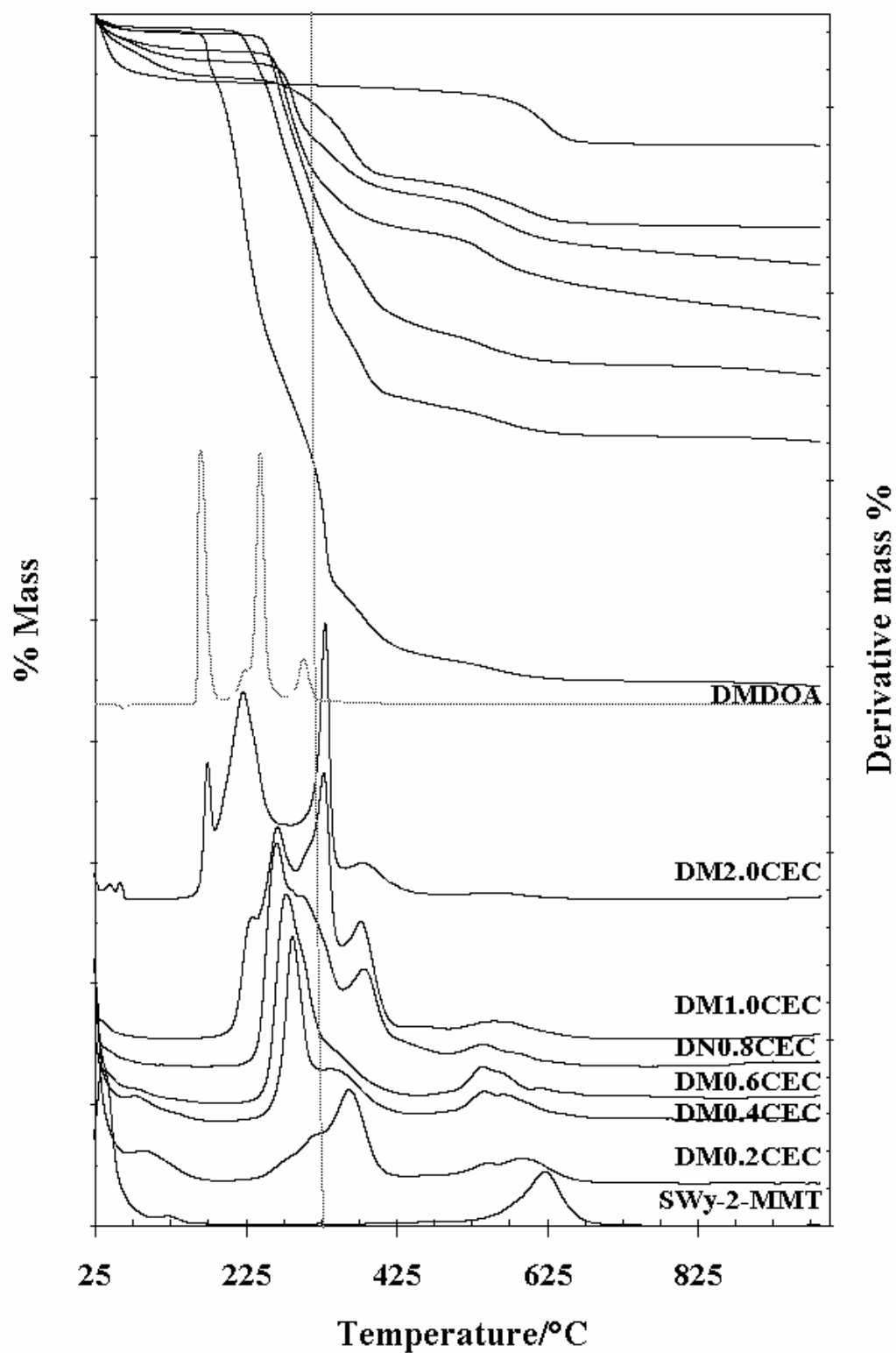


Figure 5 TG and DTG curves of DODMA modified clays

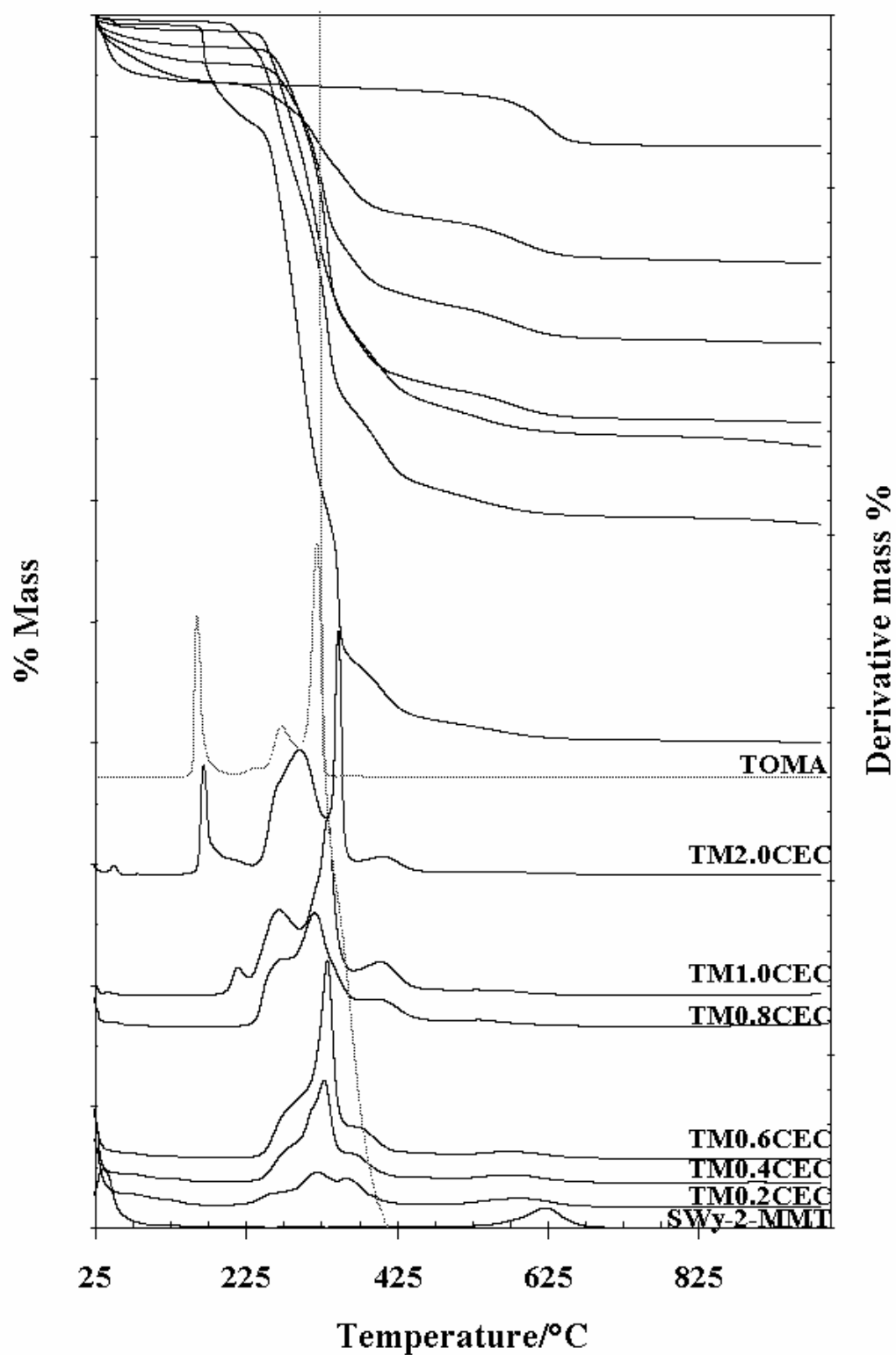


Figure 6 TG and DTG curves of TOMA modified clays

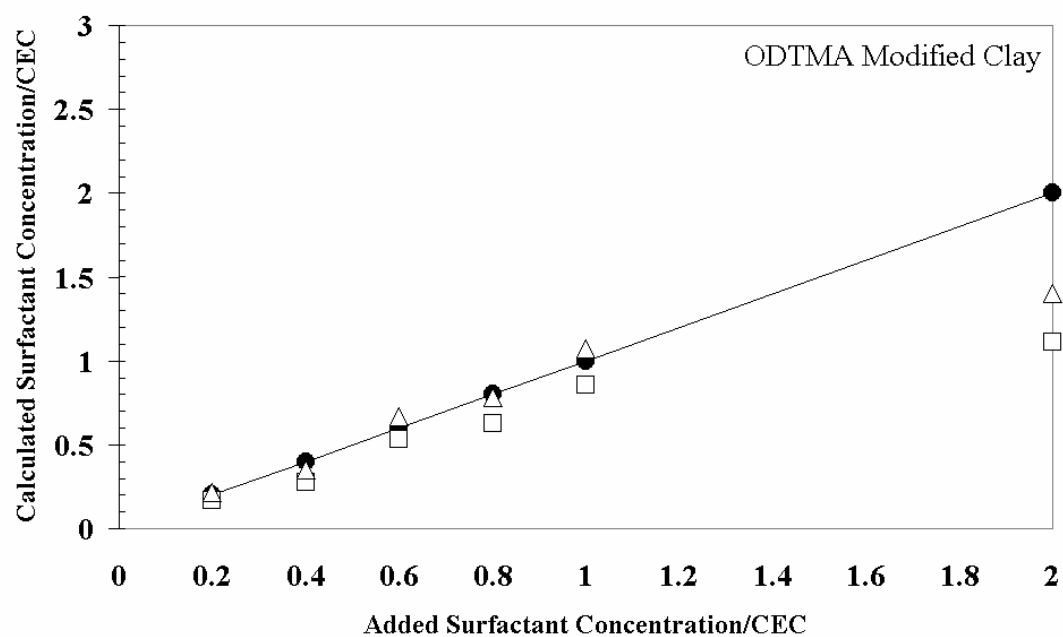


Figure 7 Real surfactant loading in ODTMA modified clays
 (solid circle represents theoretical CEC values; rectangle represents real CEC value when all Br ions remained in surfactant; triangle represents real CEC value when no Br ions remained in surfactant).

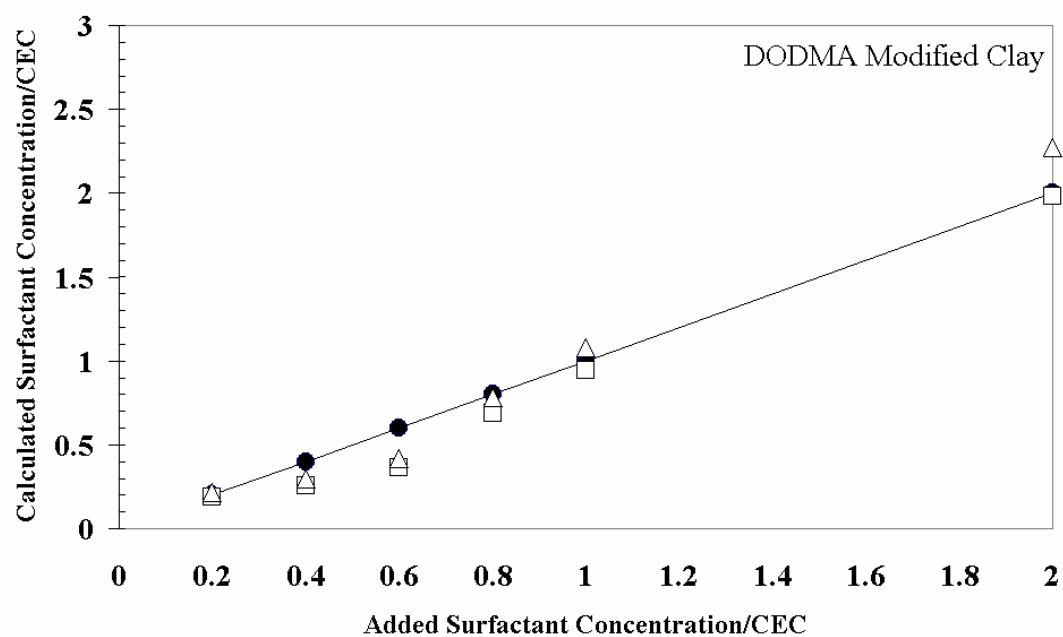


Figure 8 Real surfactant loading in DODMA modified clays
 (solid circle represents theoretical CEC values; rectangle represents real CEC value when all Br ions remained in surfactant; triangle represents real CEC value when no Br ions remained in surfactant).

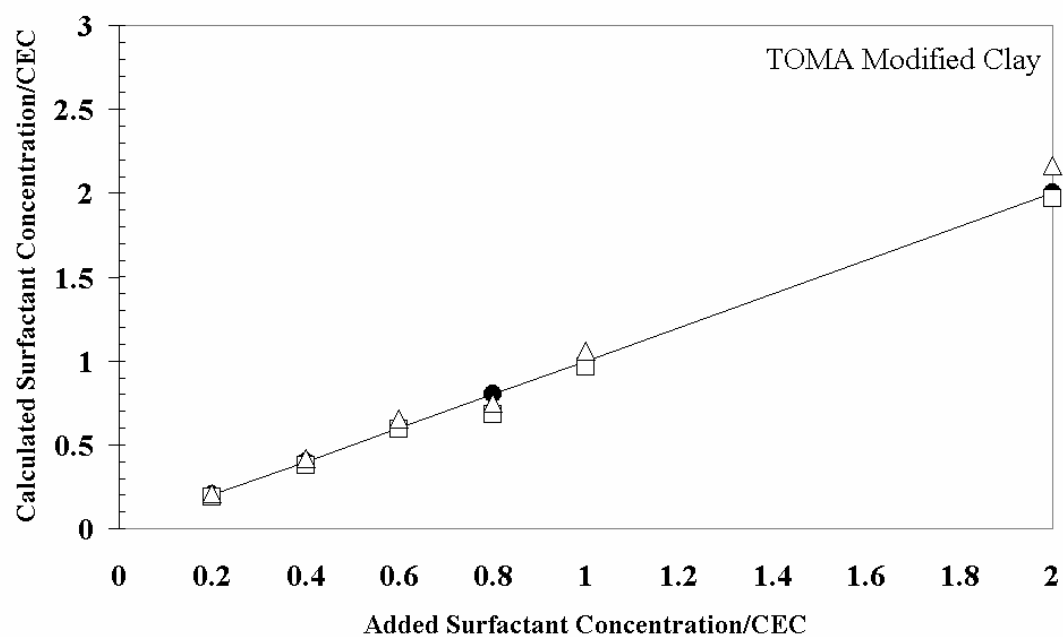


Figure 9 Real surfactant loading in TOMA modified clays
 (solid circle represents theoretical CEC values; rectangle represents real CEC value when all Br ions remained in surfactant; triangle represents real CEC value when no Br ions remained in surfactant).

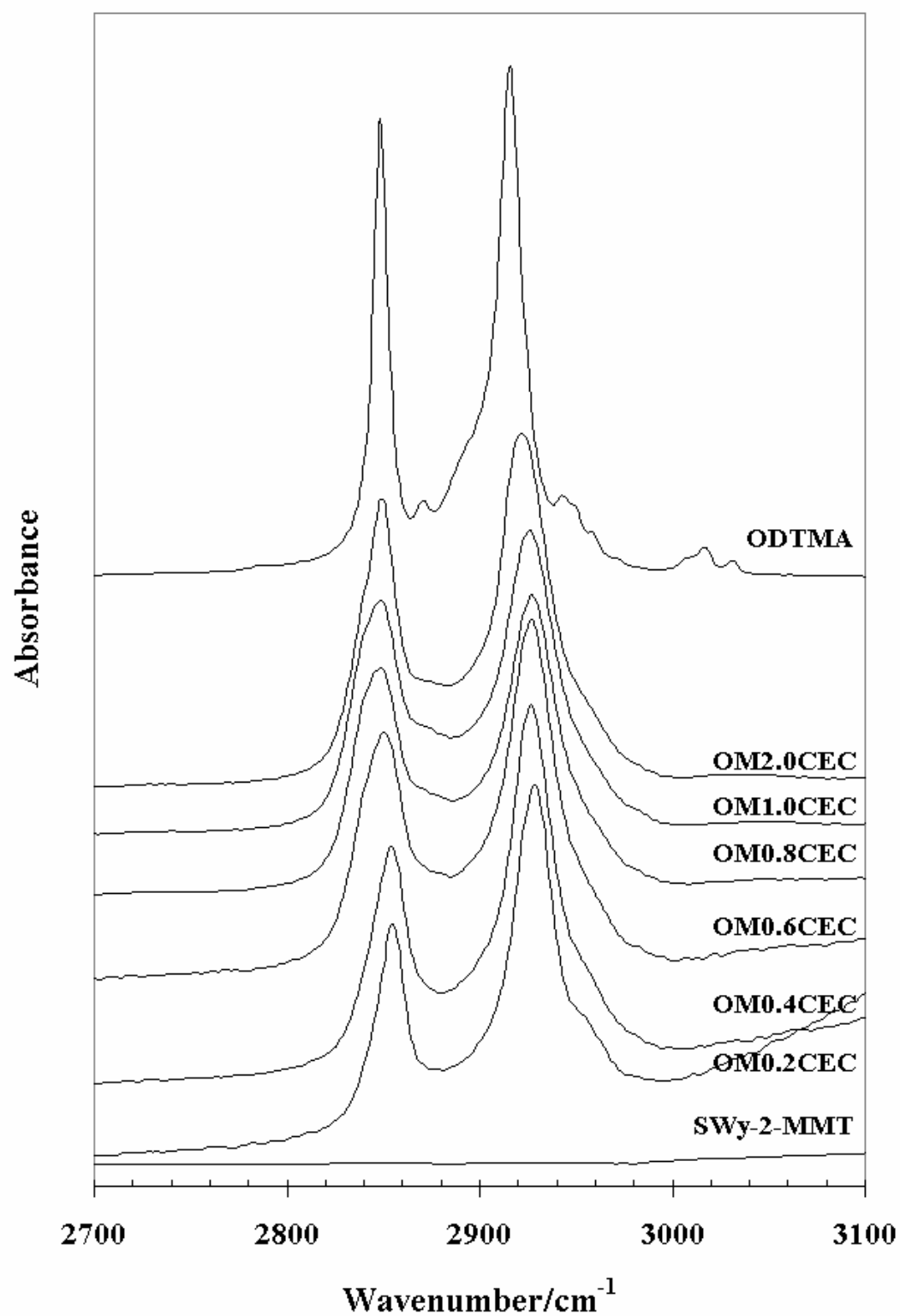


Figure 10 Antisymmetric and symmetric stretching vibrations of CH₂ in ODTMA modified clays

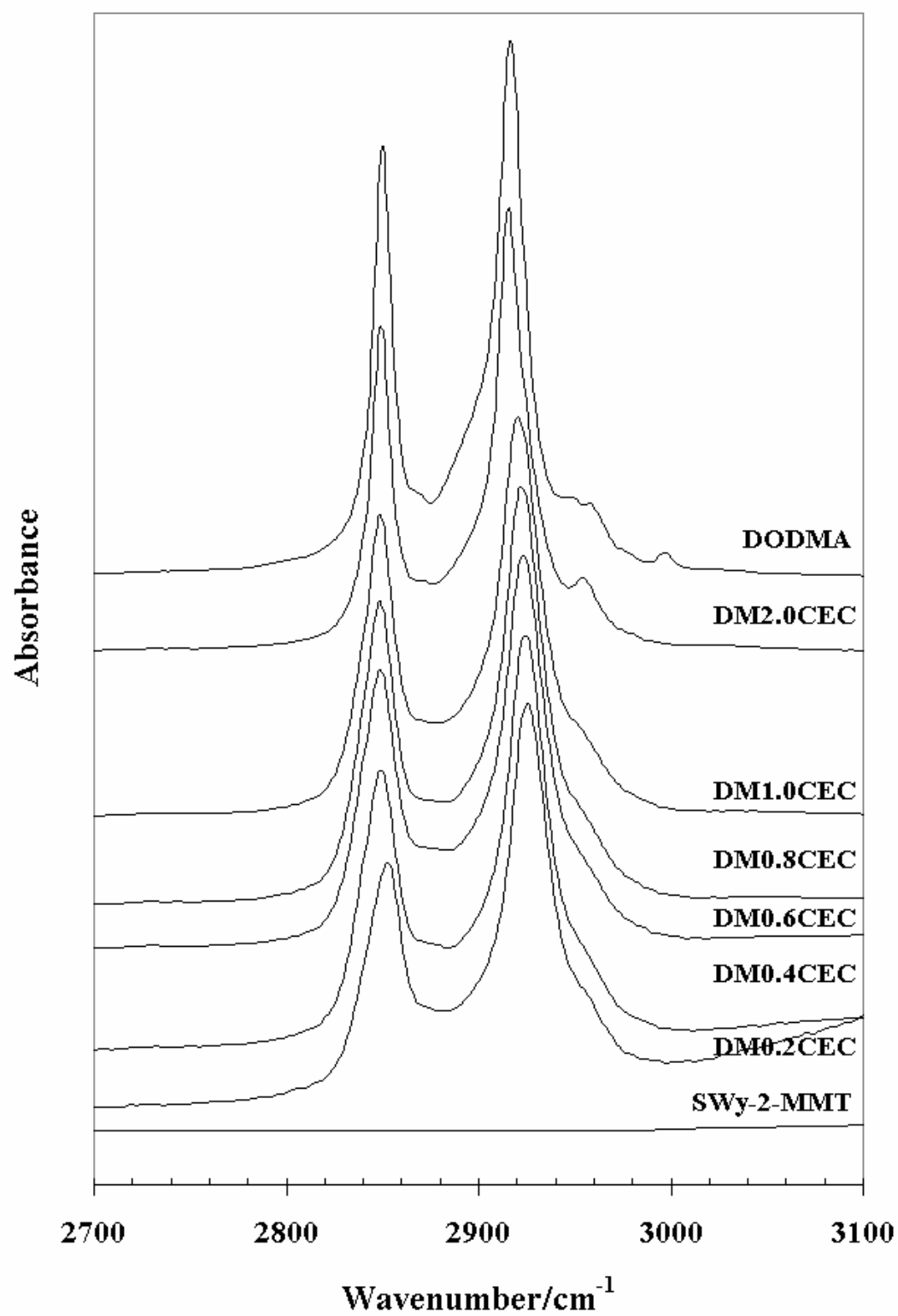


Figure 11 Antisymmetric and symmetric stretching vibrations of CH₂ in DODMA modified clays

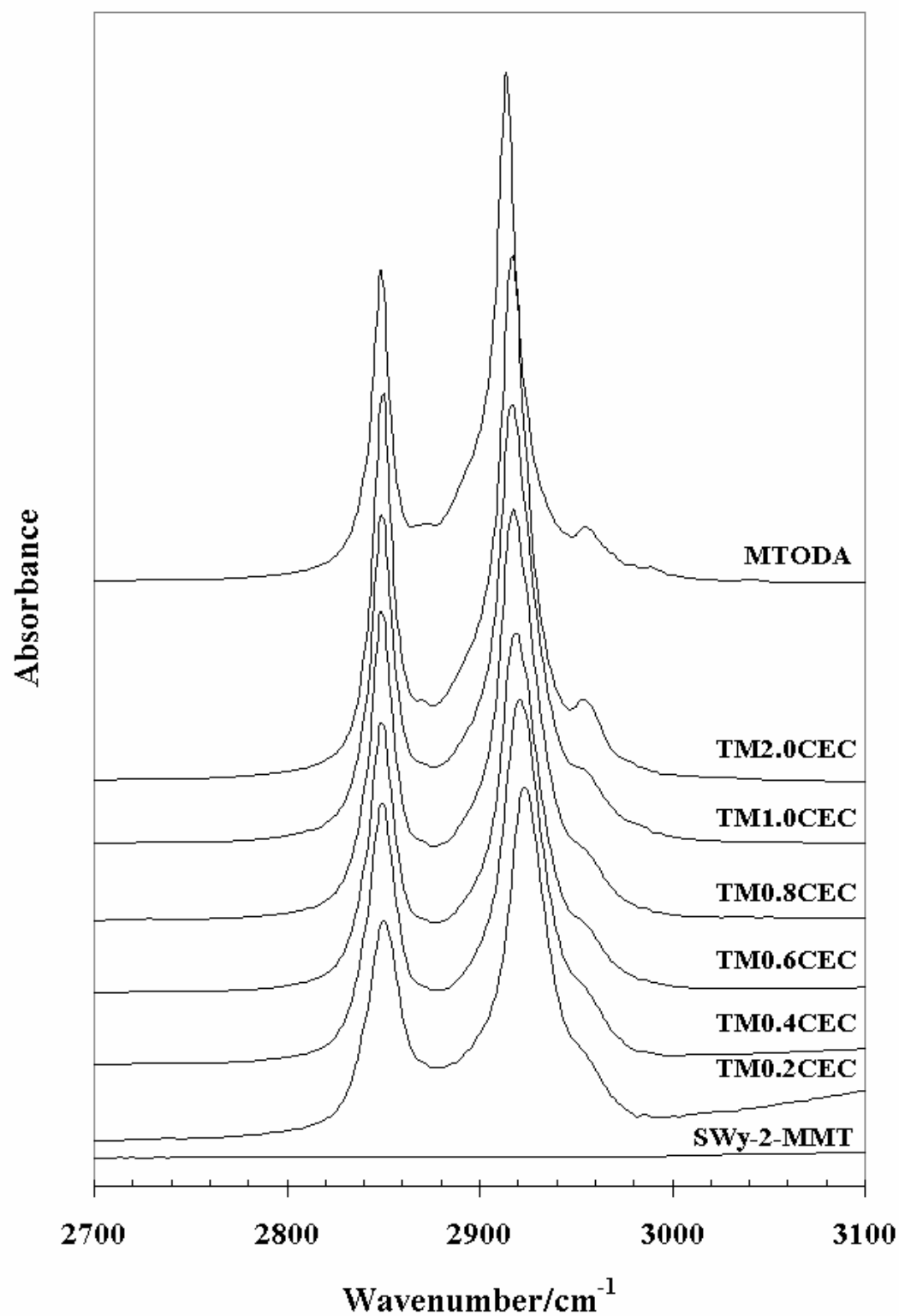


Figure 12 Antisymmetric and symmetric stretching vibrations of CH_2 in TOMA modified clays